unexposed errors. Careful consideration of potential systematic errors in the experiments reported here have produced no "smoking guns", and we have confidence in our values, D_0(HCC-H) = 131.3 ± 0.7 kcal mol^{-1} and $D_0(C_2H_3$-H) = 109.7 ± 0.8 kcal mol^{-1}. These two primary results are based on completely independent measurements. The sources of the disagreements with other experiments remain to be discovered. In the meantime, those requiring the bond energies for critical applications should consider the range of values in Tables VII and VIII. We note that improved techniques over the last 5 years have narrowed the range of experimental bond dissociation energies for acetylene and ethylene from 10–25 kcal mol^{-1} to about 5 kcal mol^{-1}.

Despite unresolved discrepancies with other experiments, the general trends shown in Table IX are certain. A large variation is observed in the CH and CC bond dissociation energies for the various molecules and radicals. A theoretical analysis of the precise magnitudes of the bond strengths in Table IX is beyond the scope of this paper, but it is useful to make some general remarks on the observed trends.

Methane, ethylene, and acetylene represent the simplest set of hydrocarbons with sp^3, sp^2, and sp hybridized carbon atoms, respectively. As expected, the CH bond dissociation energies for these molecules increase with greater s character of the bonding orbital: $D_0(CH_3$-H) = 103.24 ± 0.12 kcal mol^{-1} (ref 14), D_0-(CH_2CH-H) = 109.7 ± 0.8 kcal mol^{-1}, and D_0(HCC-H) = 131.3 ± 0.7 kcal mol^{-1}.

In the closed-shell molecules $CH_2{=}CH_2$ and HC≡CH, it is harder to break the first CH bond than subsequent CH bonds. For example, it costs 110 kcal mol^{-1} to produce the $CH_2{=}CH$ radical from ethylene, but subsequent cleavage of the vinyl α-CH bond, eq 18, requires only 81 kcal mol^{-1}. The reduced CH bond

$$CH_2{=}CH^{\bullet} \rightarrow H + CH_2{=}C: \qquad (18)$$

energy may be attributed to the singlet-coupling of the remaining electron pair, which stabilizes the singlet diradical vinylidene product, $CH_2{=}C$: ($\tilde{X}\ ^1A_1$). Removal of a CH bond from vinylidene, eq 19, uncouples the electron pair but the CC bond order

$$CH_2{=}C: \rightarrow H + HC{\equiv}C^{\bullet} \qquad (19)$$

increases upon formation of ethynyl radical. We find D_0(H-HCC) = 84 kcal mol^{-1}. In contrast, removal of the β-CH bond of vinyl, eq 20, requires merely 34 kcal mol^{-1} because it generates an

$$CH_2{=}CH^{\bullet} \rightarrow H + HC{\equiv}CH \qquad (20)$$

additional CC π bond upon formation of acetylene, as well as because the CH bonds in acetylene are stronger due to the sp hybridization. It is important to emphasize that experimental bond dissociation energies result not only from the intrinsic "strength" of the bond being broken, but also from additional stabilization or destabilization of the dissociation products. Attributing these effects to changes in the strengths of either CC bonds or CH bonds, to changes in electronic configurations (e.g., electron pairing effects or rehybridization), to resonance energies, or to some combination, is arbitrary in the absence of precise theoretical definitions.

In conclusion, these experiments demonstrate the power of gas-phase ion spectroscopy and ion kinetics techniques to determine bond dissociation energies of a variety of hydrocarbon radicals. This work also substantially improves the precision of the experimental gas-phase acidity scale between HF and H_2O.

Acknowledgment. This paper is dedicated to Professor W. Doering, who in his Cope Award address (Dallas, April 1989) lamented the fact that there seemed to be waning interest in the thermochemistry of hydrocarbons. We thank J. J. Grabowski for providing his results on the acidity of CH_2CH before publication, and we are grateful to Thom Dunning and Emily Carter for discussions concerning theoretical studies. This work was supported by grants of the National Science Foundation to C.H.D. (CHE-8815459), to V.M.B. (CHE-8815446), and to W.C.L. (CHE-8819444 and PHY-8604504), and by a grant from the U.S. Department of Energy Chemical Physics program to G.B.E. (DE-FG02-87ER13695).

Mechanistic Aspects of Decarboxylation Reactions of Group 10 $(PCy_3)_2M(H)O_2CH$ Derivatives

Donald J. Darensbourg,* Philip Wiegreffe, and Charles G. Riordan

Contribution from the Department of Chemistry, Texas A&M University, College Station, Texas 77843. *Received December 1, 1989*

Abstract: Kinetic data for the $^{13}CO_2$ exchange reactions of the *trans*-$(Cy_3P)_2M(H)O_2CH$ (M = Ni, Pd) derivatives to afford the corresponding *trans*-$(Cy_3P)_2M(H)O_2{}^{13}CH$ species are presented. These processes were found to exhibit a first-order dependence on the metal complex and to be independent of tricyclohexylphosphine or carbon dioxide concentrations. The activation parameters for the nickel complex were determined to be $\Delta H^{\ddagger}$ = 22.1 (9) kcal·mol^{-1} and $\Delta S^{\ddagger}$ = −5 (3) cal·mol^{-1}·deg^{-1}, whereas the analogous parameters for the palladium complex were found to be $\Delta H^{\ddagger}$ = 21 (2) kcal·mol^{-1} and $\Delta S^{\ddagger}$ = 4 (8) cal·mol^{-1}·deg^{-1}. The reaction pathways are proposed to proceed via rate-determining CO_2 extrusion to provide the dihydride complexes, followed by rapid $^{13}CO_2$ insertion into the M-H bond to yield the formate derivatives. Consistent with this proposal the carbon dioxide exchange rate is greater than 1200 times faster for the palladium derivative, where the $(Cy_3P)_2Pd(H)_2$ intermediate is a stable species, than for its nickel analogue, where the corresponding dihydride complex is unknown. Kinetic parameters for the intramolecular C-H/Ni-D exchange process involving *trans*-$(Cy_3P)_2Ni(O_2CH)D$ are indicative of a reaction pathway coincident with that defined for intermolecular CO_2 exchange.

Introduction

It is of importance to mechanistically understand the C-H bond forming reaction accompanying the insertion of CO_2 into transition-metal hydrides to afford metalloformates, since this is a quintessential process in carbon dioxide reductions. Although this carboxylation process or its counterpart in reverse, decarboxylation,

0002-7863/90/1512-5759$02.50/0

has been the subject of several recent theoretical treatments,[1-4] there are few kinetic studies that shed light on the reaction pathway. Most notable among the experimental investigations include those depicted in eqs 1-3. In the metalloformate described

$$(\eta^5\text{-}C_5H_5)Fe(CO)_2O_2CH \rightarrow (\eta^5\text{-}C_5H_5)Fe(CO)_2H + CO_2 \quad (1)$$

$$(\eta^5\text{-}C_5H_5)Re(O_2CH)(NO)PPh_3 \rightarrow (\eta^5\text{-}C_5H_5)Re(H)(NO)PPh_3 + CO_2 \quad (2)$$

$$fac\text{-}Re(bpy)(CO)_3H + CO_2 \rightarrow fac\text{-}Re(bpy)(CO)_3O_2CH \quad (3)$$

$$(\eta^5\text{-}C_5H_5)Fe(CO)_2O_2CH + n^{13}CO \rightleftharpoons (\eta^5\text{-}C_5H_5)Fe(CO)_{2-n}(^{13}CO)_nO_2CH + nCO \quad (4)$$

in reaction 1, ^{13}CO ligand exchange (eq 4) was shown to occur at a faster rate than decarboxylation, consistent with CO loss prior to hydrogen transfer via species **1**.[5] Presumably a vacant co-

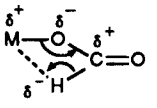

1

ordination site at the metal center is a prerequisite for hydrogen transfer from the carbon to the metal. Merrifield and Gladysz[6] have determined the activation parameters for the decarboxylation reaction 2 to be $\Delta H^{\ddagger} = 26.8$ (6) kcal·mol^{-1} and $\Delta S^{\ddagger} = -6.3$ (1.3) cal·mol^{-1}·deg^{-1}. Furthermore, this decarboxylation process has been demonstrated to proceed with retention of configuration at the metal center. While in this instance no ligand dissociation occurs on the time scale of the decarboxylation process, ring slippage or NO bending could create a vacant site at the metal center for β-hydrogen transfer.

Reaction 3 was demonstrated to be first order in both metal complex and CO_2 concentrations with activation parameters ($\Delta H^{\ddagger} = 12.8$ kcal·mol^{-1} and $\Delta S^{\ddagger} = -33.0$ cal·mol^{-1}·deg^{-1}) indicative of an I_a mechanism.[7] The transition state of the insertion reaction is proposed to have significant charge-transfer character (**1**), as revealed by the second-order rate constant varying from 1.97×10^{-4} M^{-1}·s^{-1} in THF to 5.44×10^{-2} M^{-1}·s^{-1} in CH_3CN. Consistent with sizable C-H bond formation in the transition state, reaction 3 displays an inverse isotope effect ($k_H/k_D = 0.53$). This is similarly noted in the decarboxylation reaction 2, where a kinetic isotope effect ($k_H/k_D = 1.55$) was determined.

Relevant to these processes we have reported the synthesis and reactivity of $RNi(O_2CH)(PCy_3)_2$ complexes, where R = H and Ph, and Cy = cyclohexyl.[8] In this article we present mechanistic studies of the decarboxylation reaction of $HM(O_2CH)(PCy_3)_2$ derivatives, where M is the group 10 metals Ni and Pd. This process was investigated by means of the carbon dioxide exchange reactions described in eqs 5 and 6.

$$[M]\text{-}O_2CH + {}^{13}CO_2 \rightleftharpoons [M]\text{-}O_2{}^{13}CH + CO_2 \quad (5)$$

$$D\text{-}[M]\text{-}O_2CH \rightleftharpoons DCO_2\text{-}[M]\text{-}H \quad (6)$$

Experimental Section

Methods and Materials. All manipulations were performed on a double-manifold Schlenk vacuum line under an atmosphere of dry nitrogen or in an argon-filled glovebox. Solvents were dried and deoxygenated by distillation from the appropriate reagent under a nitrogen atmosphere. Infrared spectra were recorded in 0.10-mm CaF_2 cells on an IBM IR/32 spectrometer. ^1H, ^2H, and ^{13}C NMR spectra were obtained on Varian XL-200 or -400 spectrometers. The high-pressure NMR tube was constructed in our machine shop according to the specifications of Roe.[9]

Anhydrous nickel acetylacetonate was obtained from MCB Chemicals, whereas tricyclohexylphosphine and $(\eta^3\text{-}C_3H_5)Pd_2Cl_2$ were purchased from Strem Chemicals. Trimethylaluminum and NaC_5H_5 were obtained from Aldrich, as were the deuterated solvents. Isotec, Inc. was the source of carbon-13 enriched CO_2 (99% isotope enriched). $[(Cy_3P)_2Ni]_2N_2$,[10] $(\eta^3\text{-}C_3H_5)(\eta^5\text{-}C_5H_5)Pd$,[11] and $(Cy_3P)_2Pd$[12] were synthesized according to established literature procedures with only slight modifications.

$HNi(O_2CH)(PCy_3)_2$.[13,14] Argon was passed through a solution of $[(Cy_3P)_2Ni]_2N_2$ (3.2 g, 2.5 mmol) in toluene (80 mL) until the color changed from dark-red to yellow-red. After extensive concentration of the resulting solution, addition of a solution of HCOOH (0.30 mL, 5.0 mmol) in diethyl ether (25 mL) caused yellow crystals of the desired product to precipitate in 43% yield. ^1H NMR (C_6D_6): δ 8.90 (s), -27.6 (t, $J_{HP} = 76.7$ Hz) ppm. IR (KBr): ν(NiH) 1931, ν(CO) 1619 cm^{-1}.

$DNi(O_2CH)(PCy_3)_2$. The nickel deuteride was prepared as described above by using a solution of 10% by volume HCOOH in D_2O. ^2H NMR (C_6H_6): δ -27.5 (t, $J_{DP} = 11.1$ Hz) ppm.

$HPd(O_2CH)(PCy_3)_2$. $(Cy_3P)_2Pd$ (0.400 g, 0.599 mmol) was dissolved in 20 mL of ether, and 1.0 mL (1.3 mmol) of HCOOH of a 5% by volume solution of HCOOH/methanol was added via syringe at ambient temperature. The solution was stirred for 30 min, during which time the reaction mixture turned from a white dispersion to a yellow homogeneous solution. Vacuum drying provided a gray solid in 73% yield. ^1H NMR (C_6D_6): δ 9.24 (d, $J_{HPd} = 5.2$ Hz), 2.23-1.08, -17.27 (dt, $J_{HPd} = 5.1$ Hz, $J_{Hp} = 6.3$ Hz) ppm.

Kinetic Studies of Carbon Dioxide and H/D Exchange Reactions. All kinetic investigations were performed by ^1H NMR on variable-temperature superconducting high-resolution NMR spectrometers. In a typical kinetic measurement, 15-25 mg of solid sample was weighed out inside of an argon-filled glovebox. To the solid samples was added ca. 1 mL of deuterated solvent, benzene-d_6 for kinetics in the range 15-40 °C or toluene-d_8 for lower temperatures, inside the glovebox via a disposable pipet. The solution was weighed to determine the exact quantity of solvent added and transferred to a 5-mm NMR tube. The tube was septum-sealed and removed from the glovebox, and the top was tightly sealed with paraffin. In the case of the H/D exchange reactions, NMR measurements were commenced immediately. For the CO_2 exchange reactions, the tube was cooled in a dry ice/acetone bath, evacuated for 15 s on a Schlenk line, and back-filled with ^{13}C-labeled carbon dioxide gas. For kinetic measurements below 15 °C, the reaction was quenched by immersion in a dry ice/acetone bath until NMR monitoring commenced. The first acquisition was typically started 6-8 min after addition of CO_2, the time necessary for transfer of the tube to the NMR probe, locking, and shiming. Data were taken by using an arrayed experiment file with preset pulse acquisition delay. Integrations were performed by using a first-order base-line correction program provided by Varian. The proton resonances of tricyclohexylphosphine were used as an internal integration standard. Further details for each process investigated kinetically are provided under Results.

Table I. Kinetic Data for Carbon Dioxide Exchange in $HNi(O_2CH)(PCy_3)_2$ (in C_6D_6)[a]

temp, °C	$k_{obs} \times 10^5$,[b] s^{-1}	temp, °C	$k_{obs} \times 10^5$,[b] s^{-1}
15.0	0.817	30.0	6.61
20.0	2.02	35.0	12.5[c]
25.0	3.56	40.0	20.2

[a] Reactions monitored by ^1H NMR. [b] [Ni complex] = 0.0176-0.0304 M, $P_{CO_2} = 14.7$ psi. [c] This rate constant found to be independent of added PCy_3 concentration.

(1) For molecular orbital calculations on transition-metal CO_2 complexes, see: (a) Sakaki, S.; Kudou, N.; Ohyoshi, A. *Inorg. Chem.* **1977**, *16*, 202. (b) Sakaki, S.; Kitaura, K.; Morokuma, K. *Inorg. Chem.* **1982**, *21*, 760. (c) Sakaki, S.; Dedieu, A. *J. Organomet. Chem.* **1986**, *314*, C63. (d) Sakaki, S.; Dedieu, A. *Inorg. Chem.* **1987**, *26*, 3278. (e) Mealli, C.; Hoffmann, R.; Stockis, A. *Inorg. Chem.* **1984**, *23*, 56.

(2) Sakaki, S.; Ohkubo, K. *Inorg. Chem.* **1988**, *27*, 2020; **1989**, *28*, 2583.

(3) Bo, D.; Dedieu, A. *Inorg. Chem.* **1989**, *28*, 304.

(4) Kaufmann, E.; Sieber, S.; Schleyer, P. v. R. *J. Am. Chem. Soc.* **1989**, *111*, 4005.

(5) Darensbourg, D. J.; Fischer, M. B.; Schmidt, R. E., Jr.; Baldwin, B. *J. Am. Chem. Soc.* **1981**, *103*, 1297.

(6) Merrifield, J. H.; Gladysz, J. A. *Organometallics* **1983**, *2*, 782.

(7) Sullivan, B. P.; Bruce, M. R. M.; O'Toole, T. R.; Bolinger, C. M.; Megehee, E.; Thorp, H.; Meyer, T. J. *ACS Symp. Ser.* **1988**, *No. 363*, 26.

(8) Darensbourg, D. J.; Darensbourg, M. Y.; Goh, L. Y.; Ludvig, M.; Wiegreffe, P. *J. Am. Chem. Soc.* **1987**, *109*, 7539.

(9) Roe, D. C. *ACS Symp. Ser.* **1987**, *No. 357*, 204. We are sincerely appreciative of the help Dr. C. Roe provided us during several of the fabrication stages of this extremely useful device.

(10) Jolly, P. W.; Jonas, K.; Krueger, C.; Tsay, Y.-H. *J. Organomet. Chem.* **1971**, *33*, 109.

(11) Tatsuno, Y.; Yoshida, T.; Otsuka, S. *Inorg. Synth.* **1979**, *19*, 220.

(12) Yoshida, T.; Otsuka, S. *Inorg. Synth.* **1979**, *19*, 105.

(13) The $HNi(O_2CCH_3)(PCy_3)_2$ analogue has been reported in the literature, and its synthesis was followed using formic acid in the place of acetic acid: Jolly, P. W.; Jonas, K. *Angew. Chem., Int. Ed. Engl.* **1968**, *7*, 731. An alternative less direct synthesis of this complex from CO_2 insertion into the Ni-H bond may be found in ref 8.

(14) Darensbourg, M. Y., Ludvig, M.; Riordan, C. G. *Inorg. Chem.* **1989**, *28*, 1630.

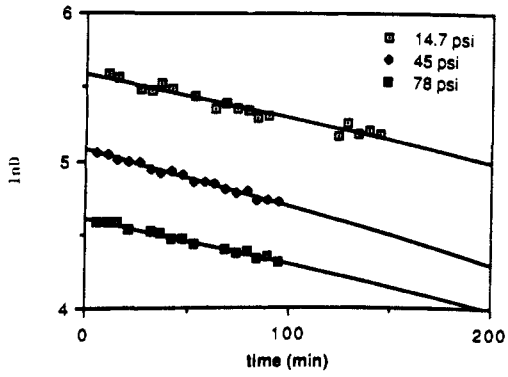

Figure 1. Effect of CO_2 concentration on the rate of reaction 7.

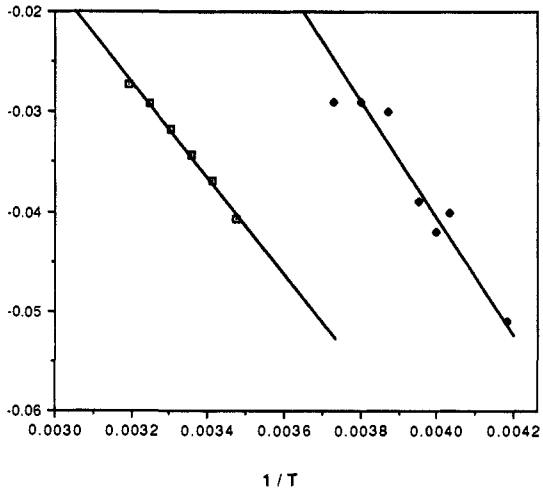

Figure 2. Erying plots for reactions 7 and 8.

Results

The carbon dioxide exchange reaction (eq 7) was effected at ambient temperature upon adding excess $^{13}CO_2$ (99% isotopically

$$\underset{\mathbf{2}}{HNi(O_2CH)(PCy_3)_2} + {}^{13}CO_2 \rightleftharpoons HNi(O_2{}^{13}CH)(PCy_3)_2 + CO_2 \quad (7)$$

enriched) to a solution of $HNi(O_2CH)(PCy_3)_2$ in C_6D_6. The decarboxylation/carboxylation reaction was monitored by both ^1H and ^{13}C NMR spectroscopy, i.e., by the gradual splitting of the formate signal at δ 8.90 ppm in the proton spectrum into a doublet centered at δ 8.90 ppm with a C–H coupling constant of 191 Hz, and the appearance of a formate carbon resonance at δ 166.8 ppm, respectively. Kinetic data as a function of temperature determined by ^1H NMR for the exchange reaction, carried out in a large excess of $^{13}CO_2$, are listed in Table I.

The exchange process indicated in eq 7 was shown to be first order in the concentration of unlabeled nickel formate complex, as indicated by the linearity of the logarithmic plot for the disappearance of [**2**] versus time (Figure 1). Concomitantly, this reaction was illustrated to be zero order in the concentration of carbon dioxide. That is, no significant changes in reaction rate were observed upon increasing the partial pressure of $^{13}CO_2$ over the range 14.7–78 psi as monitored by proton NMR (Figure 1). The addition of excess free PCy_3 has no affect on the rate of the reaction. An Erying plot of the data contained in Table I (Figure 2) provided activation parameters of $\Delta H^{\ddagger}$ = 22.1 (9) kcal·mol^{-1} and $\Delta S^{\ddagger}$ = −5 (3) cal·mol^{-1}·deg^{-1}.

The corresponding carbon dioxide exchange reaction involving palladium was likewise investigated (eq 8). This process was

$$HPd(O_2CH)(PCy_3)_2 + {}^{13}CO_2 \rightleftharpoons HPd(O_2{}^{13}CH)(PCy_3)_2 + {}^{12}CO_2 \quad (8)$$

observed to occur much faster than with its nickel analogue; hence it was necessary to measure it in the temperature range −34 to −5 °C in toluene-d_8. The reaction's progress was followed by ^1H NMR with the formate ligand in $HPd(O_2{}^{13}CH)(PCy_3)_2$ appearing as a split signal at δ 9.24 ppm (J_{CH} = 188 Hz). Rate constants for the exchange reaction, which were measured with less precision than those for the nickel formate, are provided in Table II with the Erying plot depicted in Figure 2. The derived activation parameters were $\Delta H^{\ddagger}$ = 21 (2) kcal·mol^{-1} and $\Delta S^{\ddagger}$ = 4 (8) cal·mol^{-1}·deg^{-1}. Reaction 9 was similarly followed by ^2H and ^1H

$$DNi(O_2CH)(PCy_3)_2 \underset{k_{-1}}{\overset{k_1}{\rightleftharpoons}} (DCO_2)NiH(PCy_3)_2 \quad (9)$$

NMR. This process was detected even in the solid state in an argon-filled glovebox, reaching completion in about 4 days.[15] Proton NMR of a C_6D_6 solution of $(Cy_3P)_2Ni(D)O_2CH$/$(Cy_3P)_2Ni(H)O_2CD$ demonstrated intramolecular hydrogen exchange between the hydride and formate ligands of individual molecules. The extent of reaction was calculated from the integrated intensities of the hydride and formate resonances at δ −27.6 ppm and δ 8.90 ppm, respectively. The equilibrium constant, K_{eq}, measured at 22 °C was 1.47 ± 0.04. The rate constants, $k_{obsd} = k_1 + k_{-1}$, for the approach to equilibrium determined at several temperatures from the integrated intensity ratio of the formate to hydride proton resonances as a function of time are listed in Table III, along with the corresponding values of k_1 and k_{-1}. The latter rate constants for the forward and reverse processes, k_1 and k_{-1}, were obtained from the k_{obsd} values and K_{eq}. The reaction was found to be first order in metal complex and to be characterized by $\Delta H^{\ddagger}$ = 22 (1) kcal·mol^{-1} and $\Delta S^{\ddagger}$ = −4.8 (3.5) cal·mol^{-1}·deg^{-1}. The much faster rate of decarboxylation observed for the palladium derivative precluded the synthesis of $DPd(O_2CH)(PCy_3)_2$ for an analogous kinetic investigation.

Table II. Kinetic Data for Carbon Dioxide Exchange in $HPd(O_2CH)(PCy_3)_2$ in Toluene-d_8[a]

temp, °C	$k_{obs} \times 10^5$,[b] s^{-1}	temp, °C	$k_{obs} \times 10^5$,[b] s^{-1}
−33.9	0.497	−14.9	17.3
−24.9	4.34	−9.9	43.6
−22.9	2.59	−4.9	47.2
−19.9	5.06		

[a] Reactions monitored by ^1H NMR. [b] The extrapolated rate constant at 25 °C is 4.40 × 10^{-2} s^{-1}.

Table III. Kinetic Data for Intramolecular H/D Exchange in $DNi(O_2CH)(PCy_3)_2$ in C_6D_6[a]

	rate constant × 10^5, s^{-1}		
temp, °C	k_{obs}	k_1	k_{-1}
22.0	4.48	2.66	1.82
30.0	13.2	7.84	5.36
35.0	22.4	13.4	9.00

[a] [Ni complex] = 0.050–0.179 M.

Discussion

A transition state of the form depicted in **3** for the decarboxylation reaction of $(Cy_3P)_2Ni(H)O_2CH$ (**2**) is suggested based

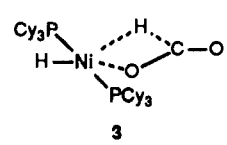

3

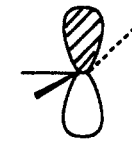

4

on the first-order dependence of the reaction on [**2**] and the zero-order dependence on carbon dioxide pressure. That is, the kinetic behavior of reaction 7 is consistent with the intermediacy of a dihydride as opposed to a diformate species. In other words, carbon dioxide extrusion preceeds carbon dioxide insertion. The spherical hydrogen 1s orbital can easily form multicenter bonds,

(15) The slower solid-state reaction probably occurs via an *intermolecular* pathway.

Scheme I

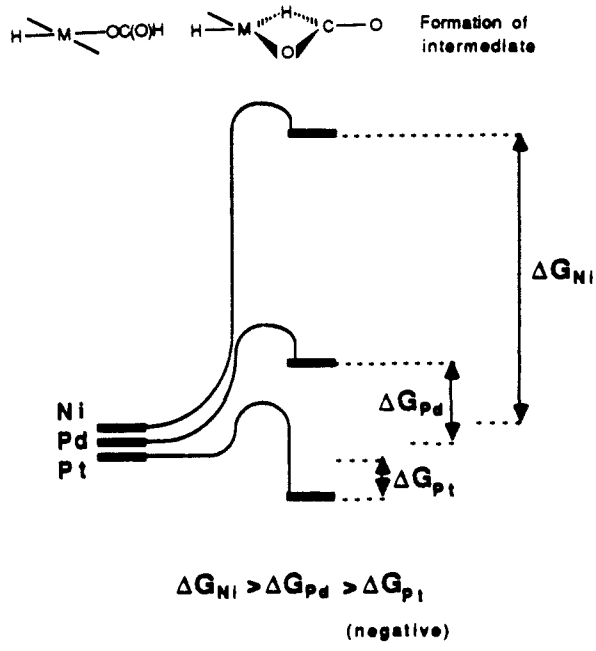

allowing it to make a nickel–hydrogen bond while breaking a carbon–hydrogen bond. Because there is a low-lying p orbital of b_2 symmetry (4) on the coordinatively unsaturated nickel center readily available for bonding with the formate ligand in an η^2-O, H chelating mode, it is unnecessary for prior loss of an ancillary ligand.[3] This is supported by the lack of inhibition of reaction 7 by the addition of excess tricyclohexylphosphine.

The activation parameters determined for this decarboxylation reaction [$\Delta H^{\ddagger}$ = 22.1 (9) kcal·mol^{-1} and $\Delta S^{\ddagger}$ = −5 (3) cal·mol^{-1}·deg^{-1}] are indicative of a transition state that involves both bond making and bond breaking. That significant metal–hydrogen bond making is occurring in **3** is best illustrated in the observation that for the analogous process involving palladium, where stronger metal–oxygen and metal–hydrogen bonds are anticipated, the reaction is some 1230 times faster at 25 °C [$\Delta H^{\ddagger}$ = 21 (2) kcal·mol^{-1} and $\Delta S^{\ddagger}$ = 4 (8) cal·mol^{-1}·deg^{-1}]. Indeed, in this instance the proposed intermediate *trans*-$H_2Pd(PCy_3)_2$ is thermally stable at ambient temperature.[16] Similarly, although the palladium dihydride is only stabilized in the presence of bulky phosphine ligands like Cy_3P, *trans*-platinum dihydrides are reported for a large variety of phosphine ligands.[17]

Hence, the stability of the dihydrides dramatically increases proceeding down the group 10 metal triad. Consequently, it would be predicted that $HPt(O_2CH)(PCy_3)_2$ would exhibit the highest reactivity toward $^{13}CO_2$ exchange. In support of this, Trogler and co-workers reported $HPt(O_2CH)(PEt_3)_2$ to exist in equilibrium with CO_2 and $H_2Pt(PEt_3)_2$ in solution.[18] In addition, $HPt(O_2CH)(PCy_3)_2$ was found to decarboxylate instantaneously upon removal of the carbon dioxide atmosphere and to recarboxylate immediately upon exposure to CO_2, even at low temperatures.[19] From the reported qualitative behavior of the $(Cy_3P)_2Pt(H)O_2CH$ complex, it can be estimated that the analogous reaction to the processes described in eqs 7 and 8 involving platinum occurs with a rate constant of >0.10 s^{-1} at 25 °C. Scheme I summarizes these observations.

The value of the equilibrium constant of 1.47 at 22 °C for eq 9 is about what is expected for an equilibrium with Ni–D and C–H bonds on the left being replaced by Ni–H and C–D on the right.[20] An equilibrium isotope effect of similar magnitude has been observed for Pt–D, C–H/Pt–H, C–D exchange.[21] Reaction 9, which formally represents an intramolecular C–H/Ni–H exchange process, by its essence must involve a CO_2 extrusion and subsequent insertion pathway. This may be concerted or stepwise in character; i.e., carbon dioxide need not leave the metal's coordination sphere as is required in the $^{13}CO_2$ exchange reaction 7 (Scheme II). Nevertheless, the similarities in the kinetic parameters for the two processes described in eqs 7 and 9 suggest a common intermediate, namely, $H_2Ni(PCy_3)_2$ or $HDNi(PCy_3)_2$. It is noteworthy that the square-pyramidal d^8 carbon dioxide complex, K[Co(R-salen)(CO_2)],[22] is experimentally known and had been theoretically studied.[1d] This complex would be analogous to the transition-state/intermediate indicated in Scheme II. In addition, the reaction of *trans*-$(Cy_3P)_2PtH_2$ with CS_2 has been demonstrated to be second order, first order each in metal complex and CS_2 concentrations, and is thought to involve a five-coordinate intermediate that rapidly inserts CS_2 to afford *trans*-$(Cy_3P)_2Pt(H)S_2CH$.[23]

Scheme II

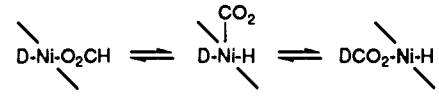

Concluding Remarks

Kinetic studies of the $^{13}CO_2$ exchange reactions of the *trans*-$(Cy_3P)_2M(H)O_2CH$ (M = Ni, Pd) derivatives indicate carbon dioxide extrusion to be rate-determining, with concomitant formation of the dihydride complex followed by rapid reincorporation of carbon dioxide. Previous qualitative observations on the platinum analogue are consistent with this reaction pathway. While these metal dihydrides are known for palladium and platinum, the corresponding nickel complex is presently unknown. In a related process, the intermediacy of $(Cy_3P)_2Ni(H)(D)$ in the C–H/Ni–D reaction involving $(Cy_3P)_2Ni(D)(O_2CH)$ is evident based on kinetic measurements.

Interestingly, attempts to extend these studies to include the *trans*-$(Cy_3P)_2Ni(Ph)O_2CH$ derivative were unsuccessful. Although *trans*-$(Cy_3P)_2Ni(Ph)O_2CH$ underwent minor amounts of $^{13}CO_2$ incorporation to afford *trans*-$(Cy_3P)_2Ni(Ph)O_2{}^{13}CH$ at ambient temperature very slowly, efforts to increase the reaction's rate by increasing the temperature led to decomposition. The slowness of this CO_2 extrusion reaction relative to the hydride analogue lends support to the importance of hydrogen interaction at the metal center in the decarboxylation process. Evidently, the crowding of the nickel site by the phenyl ligand is sufficient to induce significant retardation in the carbon dioxide extrusion process. Furthermore, there may be an electronic component to this retardation. That is, it is likely that phenyl orbitals interact with the low-lying p orbital of b_2 symmetry, making it less available for bonding with the appropriate orbital in the η^2-O, H transient. Similarly, the increase in the rate of decarboxylation of the *trans*-$(Cy_3P)_2M(H)O_2CH$ derivatives upon proceeding down the group 10 metal triad might be in part ascribed to the lowering in energy of the metal's p orbitals in going from nickel to platinum.

Acknowledgment. The financial support of this research by the National Science Foundation (Grant 88-17873) is greatly appreciated. We are obligated to the reviewers of the initial manuscript for their helpful comments.

(16) Kudo, K.; Hidai, M.; Uchida, Y. *J. Organomet. Chem.* **1973**, *56*, 413.
(17) (a) Shaw, B. L.; Uttley, M. F. *J. Chem. Soc., Chem. Commun.* **1974**, 918; (b) Immirzi, A.; Musco, A.; Carturan, G.; Belluco, U. *Inorg. Chim. Acta* **1975**, *12*, 123; (c) Leviston, P. G.; Wallbridge, M. G. H. *J. Organomet. Chem.* **1976**, *110*, 271; (d) Paonessa, R.; Trogler, W. C. *J. Am. Chem. Soc.* **1982**, *104*, 1138; (e) Packett, D. L.; Jensen, C. M.; Cowan, R. L.; Strouse, C. E.; Trogler, W. C. *Inorg. Chem.* **1985**, *24*, 3578.
(18) Paonessa, R. S.; Trogler, W. C. *J. Am. Chem. Soc.* **1982**, *104*, 3529.
(19) Immirzi, A.; Musco, A. *Inorg. Chim. Acta* **1977**, *22*, L35.
(20) Intraligand vibrations have made it difficult for us to assign the Ni–D and the C–H vibrations, hence precluding calculations of K_{eq} from ν(Ni–H), ν(Ni–D), ν(C–H), and ν(C–D) values.
(21) Rashidi, M.; Puddephatt, R. J. *J. Am. Chem. Soc.* **1986**, *108*, 7111.
(22) (a) Fachinetti, G.; Floriana, C.; Zanazzi, P. F. *J. Am. Chem. Soc.* **1978**, *100*, 7505. (b) Gambarotta, S.; Arena, F.; Floriani, C.; Zanazzi, P. F. *J. Am. Chem. Soc.* **1982**, *104*, 5082.
(23) Albinati, A.; Musco, A.; Carturan, G.; Strukul, G. *Inorg. Chim. Acta* **1976**, *18*, 219.